

Technical Note:

Modeling regional and psychophysiological interactions in fMRI: The importance of hemodynamic deconvolution

Darren R. Gitelman^{1,2,3,4}, William D. Penny⁵, John Ashburner⁵, Karl J. Friston⁵

The Northwestern Cognitive Brain Mapping Group, Cognitive Neurology and Alzheimer's Disease Center¹, Departments of Neurology², and Radiology³, Northwestern University Medical School, Chicago V.A. Healthcare System Lakeside Division⁴, Chicago, Illinois, 60611, and the Wellcome Department of Imaging Neuroscience⁵, London, UK.

To Whom Correspondence Should be Addressed:

Darren R. Gitelman, M.D.

Northwestern University Medical School

320 E. Superior St., Searle 11-470

Chicago, IL 60611

Voice: 312-908-9023

Fax: 312-908-8789

Email: d-gitelman@northwestern.edu

ABSTRACT

The analysis of functional magnetic resonance imaging (fMRI) time-series data can provide information not only about task-related activity, but also about the connectivity (functional or effective) among regions, and the influences of behavioral or physiologic states on that connectivity (Büchel and Friston, 1997). Similar analyses have been performed in other imaging modalities, such as positron emission tomography (PET) (McIntosh *et al.*, 1994). However, fMRI is unique because the information about the underlying neuronal activity is filtered or convolved with a hemodynamic response function. Previous studies of regional connectivity in fMRI have overlooked this convolution and have assumed that the observed hemodynamic response approximates the neuronal response. In this paper, this assumption is revisited using estimates of underlying neuronal activity. These estimates use a Parametric Empirical Bayes formulation for hemodynamic deconvolution.

INTRODUCTION

A common objective in functional imaging is to characterize the activity in a particular brain region in terms of the interactions among inputs from other regions or by the interaction between inputs from another region's activity and behavioral state. Examples of analyses modeling these interactions include psychophysiological interactions (PPI), physiophysiological interactions and the incorporation of moderator variables in structural equation modeling (SEM) (Büchel *et al.*, 1999; Friston *et al.*, 1997). Analyzing functional magnetic resonance imaging (fMRI) data presents a unique challenge to these techniques because the experimenter is presented with a time-series that represents the neural signal convolved with some hemodynamic response function (HRF). However, interactions in the brain are expressed, not at the level of hemodynamic responses, but at a neural level. Therefore, veridical models of neuronal interactions require the neural signal or at least a well-constrained approximation to it. Given blood oxygen level dependent (BOLD) signal in fMRI, the appropriate approximation can be obtained by deconvolution using an assumed hemodynamic response. The need for robust deconvolution is motivated neurobiologically (because brain interactions take place at a neural level) and mathematically (because modeling interactions at a hemodynamic level is not equivalent to modeling them neuronally). This note reviews the mathematical theory, presents a simple method for constrained deconvolution, and demonstrates the method using simulated and empirical datasets.

THEORY

Brain interactions occur at a neuronal level, yet the signal observed in fMRI is the hemodynamic response engendered by that neuronal activity. The problem is how to construct regressors,

based on hemodynamic observations, which model neuronal influences. The hemodynamic response to neural activity can be modeled by convolution with a finite impulse response function

$$y_t = \sum_{\tau} h_{\tau} x_{t-\tau} \quad (1)$$

where y_t is the measured BOLD signal at time t , h_{τ} is the hemodynamic response function defined at times τ , and $x_{t-\tau}$ is the neuronal signal at time t minus τ . This equation can be reformulated in matrix notation as

$$y = Hx \quad (2)$$

where H is the HRF in Toeplitz matrix form.

Assume that we wish to model the interaction between neural activities in two areas. Given the bold signal from two regions y_A and y_B we might try taking the product at each point in time to generate the interaction term; however, this would not produce the signal induced by interactions at a neuronal level (i.e., x_A and x_B representing neuronal activity from two regions), since we have neglected convolution with the HRF. This can be expressed mathematically for BOLD responses (3), and for the interaction of a psychological variable with BOLD signal (4).

$$y_A y_B = (Hx_A)(Hx_B) \neq H(x_A x_B) \quad (3)$$

$$HPy_A = (HP)(Hx_A) \neq H(Px_A) \quad (4)$$

The proper form of the necessary physiologic variables (e.g., x_A) must first be obtained from the observed BOLD activity (e.g., y_A). The first step is to expand x_A in terms of a temporal basis set X such as a Fourier set or a set of cosine functions

$$x_A = X\beta \quad (5)$$

where β are parameters that control the expression of different frequency components of x_A . Introducing observation noise, we create a linear model whose maximum likelihood estimators are obtained through the Gauss-Markov theorem

$$y_A = HX\beta + \varepsilon \quad (6)$$

$$\hat{\beta}_{ML} = (X^T H^T \Sigma^{-1} HX)^{-1} X^T H^T \Sigma^{-1} y_A \quad (7)$$

where $\varepsilon \sim N(0, \sigma^2 \Sigma)$, σ^2 is the error variance, and Σ is the error correlation matrix. Using the estimates, $\hat{\beta}_{ML}$, one could then derive the neural signal for each BOLD vector and compute the required interaction terms using the left hand expressions in equations 3 or 4.

However, estimates based on a full-rank basis set are generally very inefficient (i.e., highly variable). This is particularly so for the coefficients in $\hat{\beta}$ controlling high frequencies, because the HRF selectively attenuates high frequencies. The estimates therefore have to be constrained or regularized. This could be achieved, for example, by setting the high-frequency estimates to zero by removing high-frequency terms from the basis set. This would give a least squares maximum likelihood deconvolution that is motivated by smoothness constraints on the solution. Constraints like this could also be implemented using a Bayesian formulation in which the estimated neuronal activity conforms to a Bayesian estimator with priors on its frequency structure. The advantage of the Bayesian formulation is that it allows a more flexible specification of the priors. The corresponding Bayesian estimator (under Gaussian assumptions) is

$$\hat{\beta}_{MAP} = (X^T H^T \Sigma^{-1} HX + \sigma^2 C_\beta^{-1}) X^T H^T \Sigma^{-1} y_A \quad (8)$$

where $\hat{\beta}_{MAP}$ is the maximum a posteriori estimate, and C_β^{-1} is the prior precision (inverse of the prior covariance) of β . By setting the leading diagonal elements of C_β^{-1} corresponding to the highest frequencies to infinity (i.e., these coefficients have zero mean and variance) the solution is effectively restricted to lower frequencies. This would render (8) equivalent to the least squares deconvolution described above that obtains after removing the highest frequencies from X .

.

e.g.

$$C_\beta = \begin{bmatrix} \infty & \cdots & 0 & 0 \\ \vdots & \ddots & \vdots & \vdots \\ 0 & \cdots & \infty & 0 \\ 0 & \cdots & 0 & 0 \end{bmatrix} \Rightarrow C_\beta^{-1} = \begin{bmatrix} 0 & \cdots & 0 & 0 \\ \vdots & \ddots & \vdots & \vdots \\ 0 & \cdots & 0 & 0 \\ 0 & \cdots & 0 & \infty \end{bmatrix}$$

This Bayesian formulation is potentially useful because it accommodates more finessed regularizations than simply removing columns from X . The simplest constraint (used in the examples below) is to assume the underlying neuronal process is white, with the uniform expression of all frequencies:

$$e.g. \quad C_\beta = \lambda \begin{bmatrix} 1 & 0 & \cdots & 0 \\ 0 & 1 & & \vdots \\ \vdots & & \ddots & 0 \\ 0 & \cdots & 0 & 1 \end{bmatrix} = \lambda Q \quad (9)$$

This is a more graceful form of constraint in which all frequencies are estimated, but in a way that ensures the frequency profile conforms roughly to spectral profile specified in the prior covariances. Note that we have introduced a hyperparameter λ that controls the variance, given that the relative variances conform to the leading diagonal of Q . We could assume a particular value for λ based on expectations about the variance of x_A . This would render $\hat{\beta}_{MAP}$ a fully Bayesian estimator. However, it is difficult to specify λ for all situations, and a more flexible approach is to estimate it from the data. This leads to empirical Bayes estimators. Then λ can be estimated using restricted maximum likelihood (ReML) as described in Friston *et al.* (in press) using a simple hierarchical observation model and expectation-maximization (EM)

$$\begin{aligned} y_A &= HX\beta + \varepsilon^{(1)} \\ \beta &= 0 + \varepsilon^{(2)} \end{aligned} \quad (10)$$

where, as before, $\text{cov}(\varepsilon^{(1)}) = \sigma^2 \Sigma$ is the variance of the observation error and $\text{cov}(\varepsilon^{(2)}) = \lambda Q = C_\beta$ is the prior covariance of β which enters into (8) to give $\hat{\beta}_{MAP}$ (Friston *et al.*, in press). Finally, $\hat{\beta}_{MAP}$ can then be used to calculate \hat{x}_A and form the appropriate interaction terms for statistical modeling.

EXAMPLES

To illustrate the importance of deconvolving prior to forming interactions we will use the interaction between two simulated event-related responses. Note that all deconvolutions in this paper employed a discrete cosine transform basis set, and a white noise form for the prior constraints on C_β . The simulated data consisted of 115 scans, with a TR of 2 seconds. Figure 1A shows 20 event-related neural responses during a 230 second scanning session. Neural responses were formed by convolving a stick function with an exponential decay having a time constant of 1000 msec. Figure 1B shows responses to the same events from a different area. The only difference between the two regions was the trial-to-trial latency in neural activity that varied uniformly between 0 and 8 seconds. Simulated neural activities from these two regions convolved with a HRF are shown in figure 1C and 1D respectively.

INSERT FIGURE 1

The result of multiplying the hemodynamic responses, in these two regions, to generate the interaction term is shown in figure 2A. In contrast, figure 2B shows the result of first obtaining neural signals by deconvolution, multiplying the neural signals to obtain the interaction term, and then reconvolving with a HRF. The results of these operations are clearly different because the interaction term in figure 2A is completely insensitive to the relative onsets of the neuronal activities that determine the degree of interaction.

INSERT FIGURE 2

The simulated BOLD data were noise free, whereas actual BOLD data contain a substantial amount of noise, which could affect parameter estimation. To model observation error the standard deviations of the simulated BOLD data were calculated and Gaussian noise was added to the simulated BOLD signal. The original and deconvolved noise free neuronal signals are shown in figure 3A. The effects of adding 25%, 50% and 100% Gaussian noise on the deconvolution is shown in figure 3B – D. The addition of Gaussian noise results in a relative loss of high frequency components. This is because the Bayesian estimator depends more on the priors as the level of noise increases.

INSERT FIGURE 3

To examine the effects of noise on the hemodynamic and neural interactions, neural event vectors were constructed with 35 events. These vectors were then treated as outlined above, including convolution with a HRF, addition of Gaussian noise, generation of the hemodynamic interaction, deconvolution of the individual hemodynamic responses, generation of the neuronal interaction, and reconvolution of the neuronal interaction with a HRF. Noise effects on the BOLD versus neuronal interactions are shown in figure 4.

INSERT FIGURE 4

The hemodynamic interactions (top panels) are much more affected by adding noise than the neuronal interactions (lower panels). This example was chosen to make the distinction between interactions at the neuronal and hemodynamic levels very apparent. In practice, the distinction may be less pronounced because experimentally induced changes in neuronal activity have fewer high frequency components, which attenuates the impact of the convolution. The hemodynamic regressors in figures 2 and 4 are still valid regressors but the interactions they model are at the hemodynamic, not the neuronal, level. In fact, the analysis of non-linearities in hemodynamic responses presented in Friston et. al. (1998) used these sorts of regressors to estimate second order Volterra kernels.

An application to empirical BOLD data is shown in figures 5 and 6. The data in figure 5 were taken from a lexical decision task (Gitelman, unpublished data), while the data in figure 6 are from a task of covert spatial attention (Gitelman, unpublished data). As noted previously, real data may show less pronounced differences between BOLD versus neuronal interactions because there are fewer high frequency components particularly, when block design data are used. As anticipated the disparities between BOLD and neuronal interactions for event related designs (Figure 5) are moderated in block designs (Figure 6). The Pearson correlation coefficient for the BOLD versus neuronal interaction for block design data ($r = 0.948$) was significantly better than that for event-related data ($r = 0.709$), based Fisher's Z-transformation ($z = 7.27$, $p < 0.00000001$).

INSERT FIGURES 5 and 6

CONCLUSION

This paper has illustrated the distinction between interactions among BOLD signals as opposed to interactions occurring at a neuronal level. When modeling neural networks, interactions occur at a neuronal level, thus, it is important to generate the proper form of the interaction term. The distinction between BOLD and neuronal interactions appears to be even more prominent in the setting of high noise, further demonstrating the importance of deconvolution for generally noisy fMRI data. Although there are potentially, simpler methods for deconvolution, such as using least squares, these methods provide rather harsh constraints and may show distortions with noisy data. We have motivated the use of a parametric empirical Bayesian formulation in order to generate well-constrained priors on the basis set, allowing the specification of prior in terms of the frequency structure of fMRI data.

ACKNOWLEDGMENTS

DRG was supported by a grant from the NIA (K23 00940-03). WBP, JA, and KJF were supported by the Wellcome Trust.

REFERENCES

- Büchel, C. and Friston, K. J. 1997. Modulation of connectivity in visual pathways by attention: cortical interactions evaluated with structural equation modeling and fMRI. *Cereb. Cortex*. **7**: 768-778.
- Büchel, C., Coull, J. T. and Friston, K. J. 1999. The predictive value of changes in effective connectivity for human learning. *Science* **283**: 1538-1541.
- Friston, K. J., Buechel, C., Fink, G. R., Morris, J., Rolls, E. and Dolan, R. J. 1997. Psychophysiological and modulatory interactions in neuroimaging. *NeuroImage* **6**: 218-229.
- Friston, K. J., Josephs, O., Rees, G. and Turner, R. 1998. Nonlinear event-related responses in fMRI. *Mag. Res. Med.* **39**: 41-52.
- Friston, K. J., Penny, W., Phillips, C., Kiebel, S., Hinton, G. and Ashburner, J. in press. Classical and Bayesian inference in neuroimaging: Theory. *NeuroImage*.
- McIntosh, A. R., Grady, C. L., Ungerleider, L. G., Haxby, J. V., Rapoport, S. I. and Horwitz, B. 1994. Network analysis of cortical visual pathways mapped with PET. *J. Neurosci.* **14**: 655-666.

Figure Legends

Figure 1: Neural activity from twenty simulated neural events is displayed. The signal level in all figures has been normalized and displayed in arbitrary units (au). The activity from area B (1B) has been slightly and variably delayed in relation to the activity from area A (1A). Neural activity was produced by randomly generating twenty delta functions and convolving them with an exponential decay function. C and D illustrate simulated noiseless BOLD signal generated by convolving the neural activity with a HRF.

Figure 2: A) Interaction term produced by multiplying BOLD signal A with BOLD signal B. Note this interaction is in terms of hemodynamic activity, not neural activity. B) Interaction term produced by deconvolving the HRF from BOLD signal from A and B, multiplying the resulting estimated neural activities and reconvolving with a HRF. Note the difference between the interactions.

Figure 3: The effect of noise on the deconvolution. A) Plot of original (dotted line) and deconvolved (solid line) noiseless simulated BOLD data. The effect of adding Gaussian noise, 25% to 100%, is illustrated in B – D.

Figure 4: Hemodynamic interactions in the setting of 0% and 100% Gaussian noise is shown in 4A and 4B. Deconvolved neuronal interactions in the setting of 0% and 100% Gaussian noise is illustrated in 4C and 4D respectively

Figure 5: Psychophysiological interactions from an event-related fMRI data. A) event-related BOLD signal (black) and regenerated BOLD signal (red). The regenerated signal was produced by deconvolving the BOLD signal using the techniques in this report, and then reconvolving with a HRF in order to compare the result of the deconvolution procedure with the original signal. B) psychological variable; C) Hemodynamic interaction; D) Neuronal interaction.

Figure 6: Psychophysiological interactions from a block-design experiment. A) block-design BOLD signal (black) and regenerated BOLD signal (red). The regenerated signal was produced as for figure 5. B) psychological variable; C) Hemodynamic interaction; D) Neuronal interaction.

Figure 1

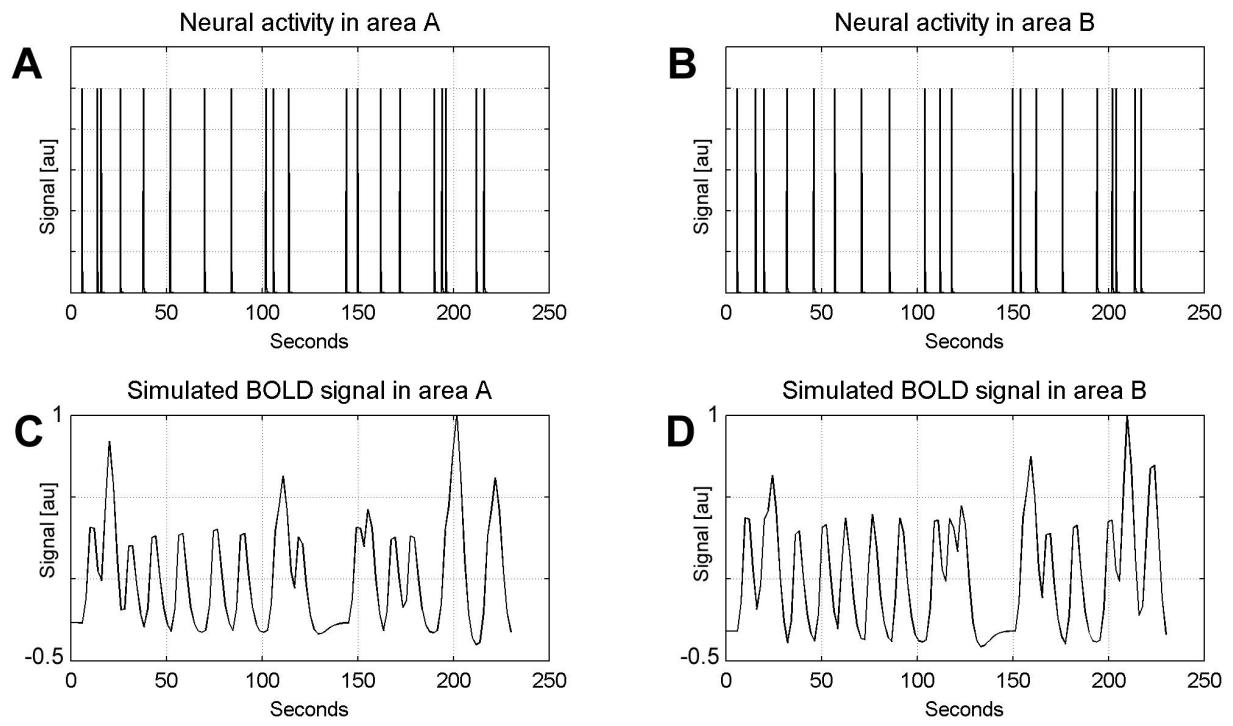


Figure 2

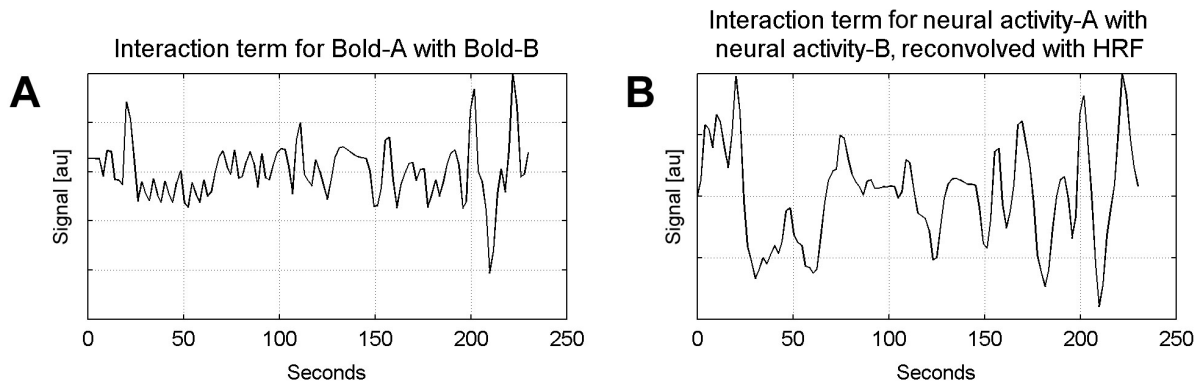


Figure 3

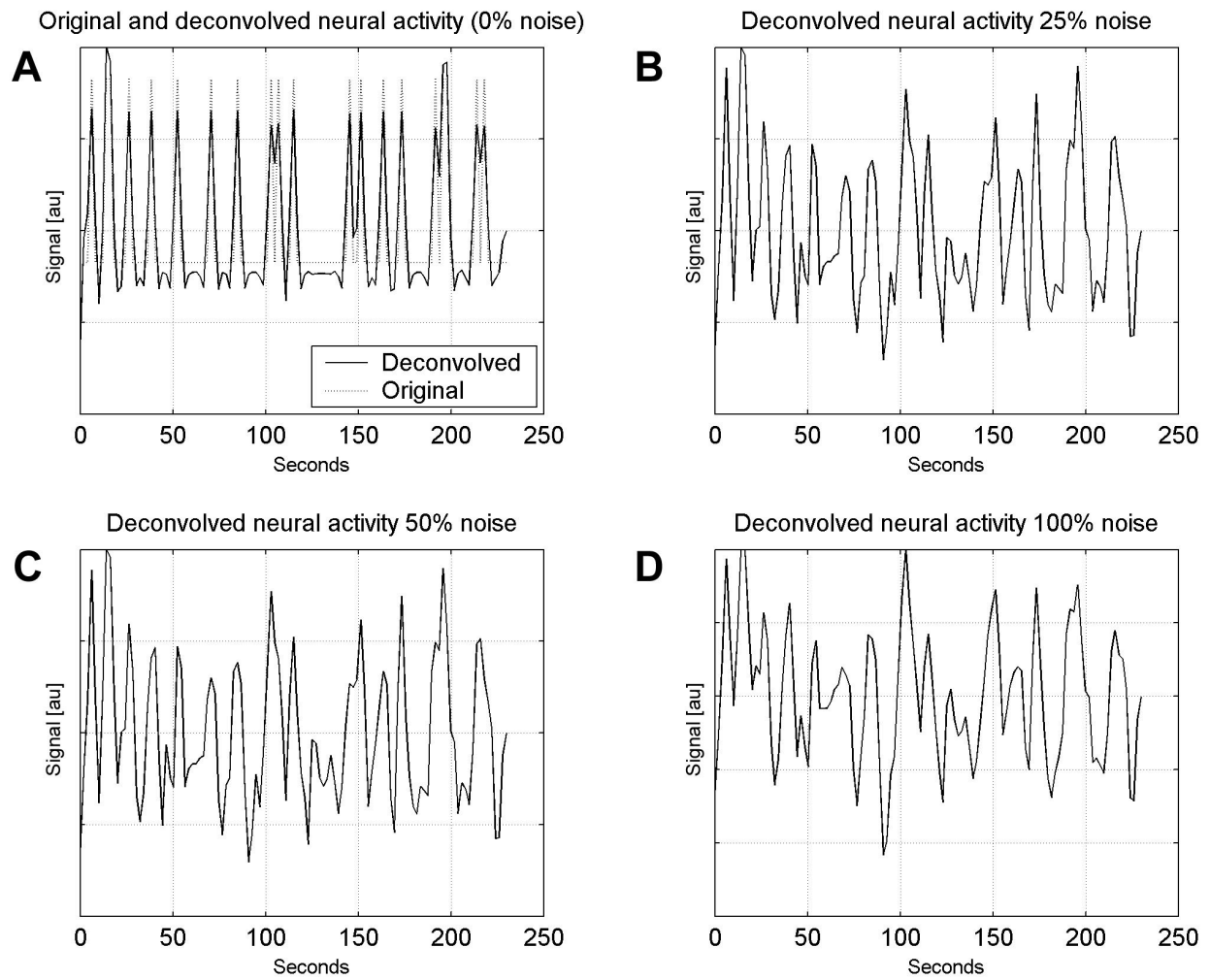


Figure 4

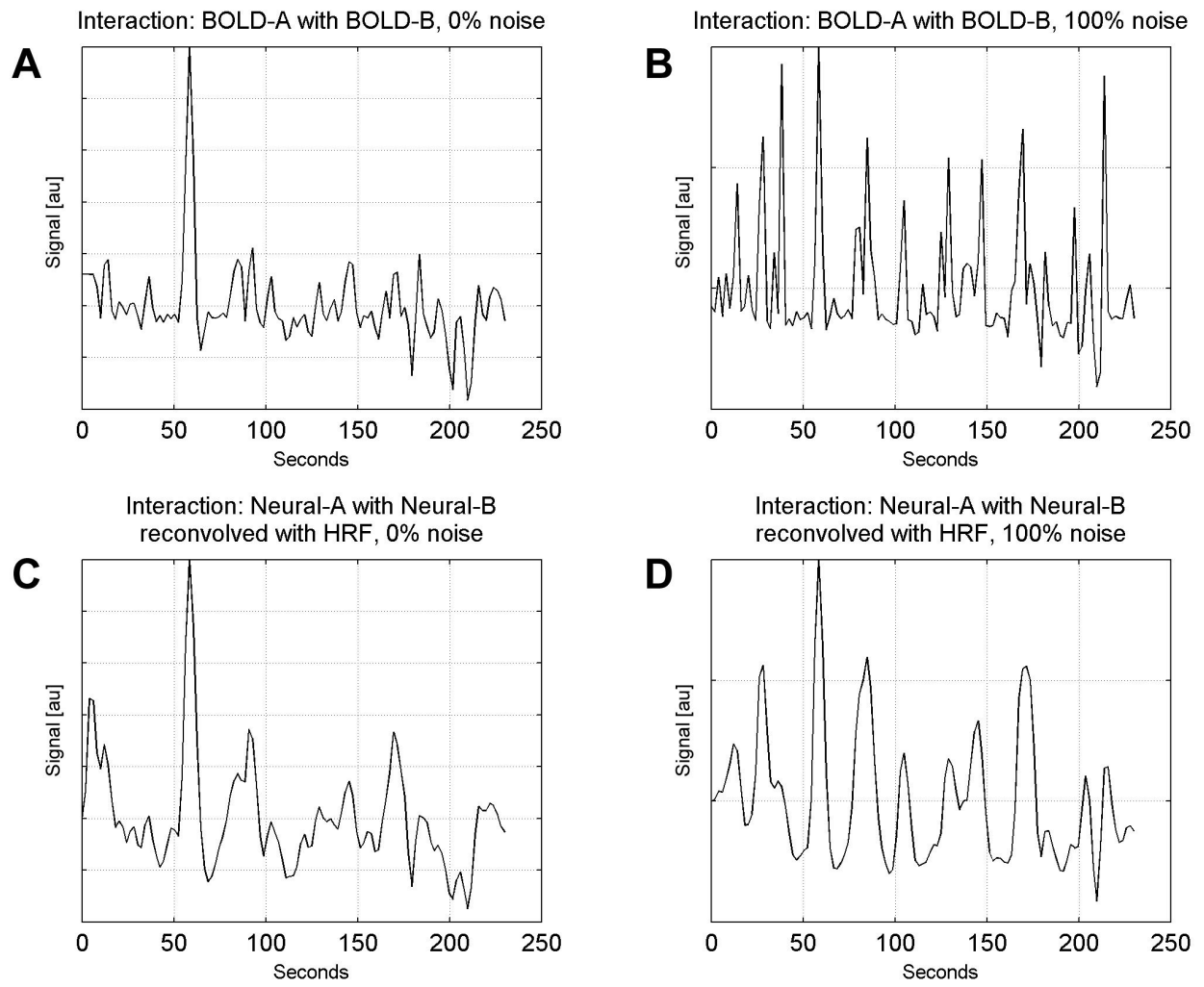


Figure 5

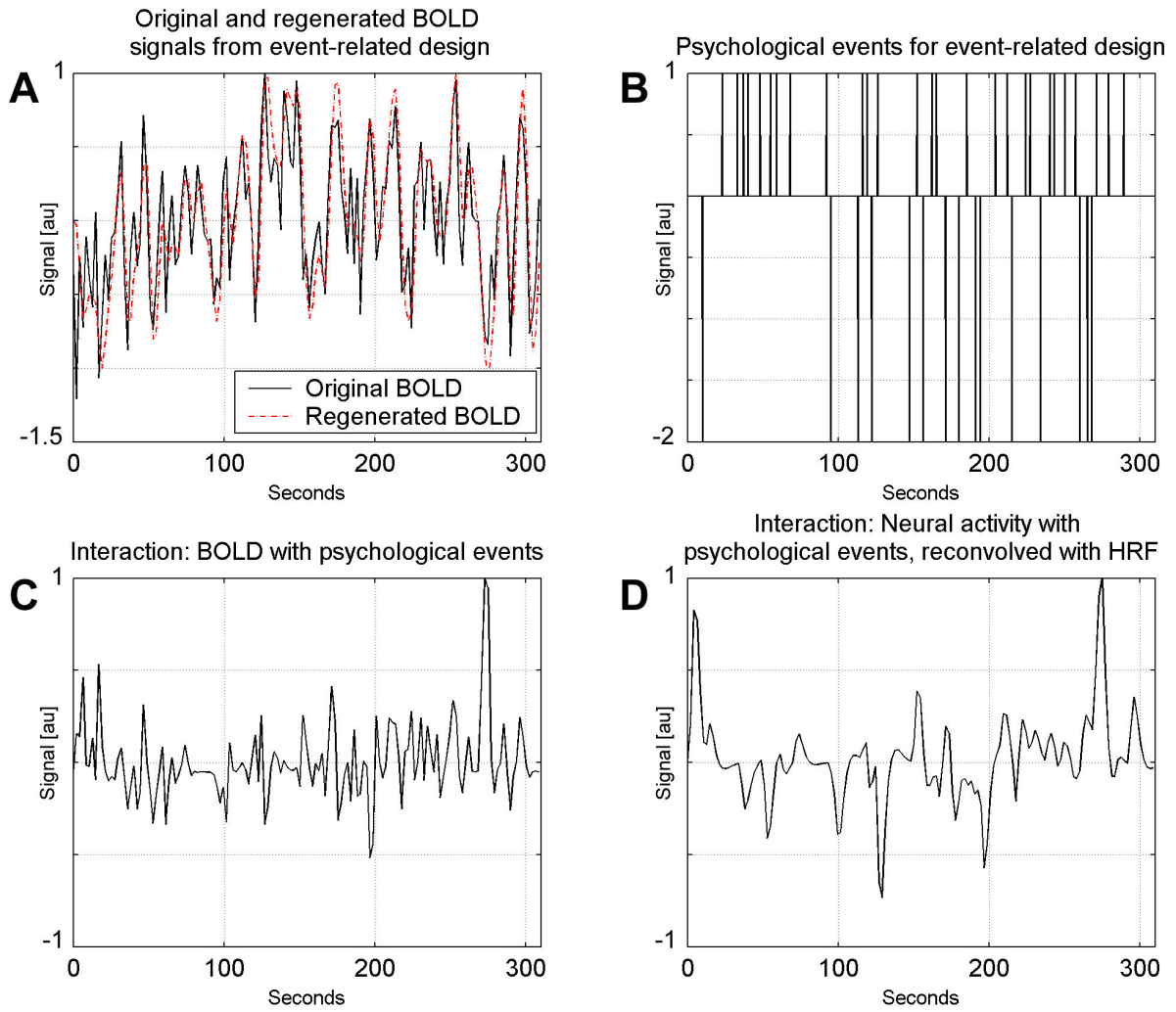


Figure 6

